

## PALLADIUM-SUPPORTED CATALYSTS IN METHANE COMBUSTION. COMPARISON OF ALUMINA AND ZIRCONIA SUPPORTS

Daniela Domingos, Lílian Maria Tosta Simplicio Rodrigues\*, Soraia Teixeira Brandão, Maria da Graça Carneiro da Rocha e Roger Frety

Instituto de Química, Universidade Federal da Bahia, Rua Barão de Geremoabo, s/n, Campus de Ondina, 40170-290 Salvador – BA, Brasil

Recebido em 4/8/11; aceito em 6/2/12; publicado na web em 15/5/12

Palladium catalysts supported on alumina and zirconia were prepared by the impregnation method and calcined at 600 and 1000 °C. Catalysts were characterized by BET measurements, XRD, XPS, O<sub>2</sub>-TPD and tested in methane combustion through temperature programmed surface reaction. Alumina supported catalysts were slightly more active than zirconia supported catalysts, but after initial heat treatment at 1000 °C, zirconia supported palladium catalyst showed better performance above 500 °C. A pattern between temperature interval stability of PdO<sub>x</sub> species and activity was observed, where better PdO<sub>x</sub> stability was associated with more active catalysts.

Keywords: palladium; zirconia; methane combustion.

### INTRODUCTION

In the pertinent literature on catalytic combustion of methane, either for low temperature applications such as the removal of traces of methane in the exhaust gases of lean burn natural gas vehicles, or for high temperature applications such as turbine actuation, palladium catalysts have been confirmed as one of the most efficient materials.<sup>1-9</sup> Some reasons for this include: palladium-based catalysts are extremely active in methane oxidation which guarantees ignition at low temperatures (below 400 °C); palladium species formed under reaction conditions (up to 800 °C) present low volatility; these systems have the unique capability of temperature self-control associated with the reversible PdO (active)/Pd (inactive) transformation.

The nature of the support, chemical state, and palladium particle size play an important role in the catalytic behavior of these systems.<sup>10,11</sup> The role of the support has been widely studied in the literature<sup>7,12-17</sup> and it has been concluded that the catalytic properties of palladium depend on the nature of the support, which influences palladium-support interaction. Among the various supports used, alumina and zirconia have been the most studied.<sup>1,3-5,9,11,13,17-24</sup>

The support most commonly used for Pd catalysts is alumina and many studies focusing on Pd/alumina catalysts are available.<sup>10,11,18</sup> However, alumina is not fully stable at the high temperatures reached in methane combustion as it undergoes a phase change at 800 °C from  $\gamma$ -alumina to  $\delta$ -alumina, resulting in a loss of surface area.<sup>23</sup> Hoflund *et al.*<sup>24</sup> studied CeO<sub>2</sub>, ZrO<sub>2</sub> and MnO<sub>2</sub> as supports in nanocrystalline and polycrystalline form. These authors found that nanocrystalline ZrO<sub>2</sub> and CeO<sub>2</sub> supports showed appreciable activities below 300 °C. ZrO<sub>2</sub> has also been used as a support by other researchers.<sup>20-22</sup>

With respect to the active phase, a number of studies<sup>20,25-30</sup> have attempted to define the chemical state of the active phase of the palladium species during catalytic combustion, and it is generally agreed that PdO<sub>x</sub> species are essential, at least below 700-800 °C, where PdO<sub>x</sub> species should be thermodynamically stable. Whether metallic palladium is also permanently present for the dissociative adsorption of methane or participates in the catalytic cycle, formed

by the reduction of PdO<sub>x</sub> by methane and destroyed by reoxidation with oxygen, remains a matter of debate.

More recently, studies using *in situ* observation techniques such as XANES, high temperature XRD and Raman spectroscopy under catalytic conditions, have clearly shown that palladium activity increases when PdO<sub>x</sub> species are formed and decreases when metallic palladium appears.<sup>31,32</sup> However, these techniques are unable to detect traces of either chemical states of palladium. Due to the fact that PdO<sub>x</sub> is necessary for good catalytic activity, various studies have examined the possibility of controlling and changing PdO<sub>x</sub> stability, firstly by altering the support material and mean particle diameter of the palladium species, secondly by introducing promoters either on the metal or in the support, and lastly by using a large number of preparation techniques. No clear conclusions have yet been drawn from these studies: quantitative amounts of oxidized palladium cannot be linked directly to catalytic activity.

The aim of the present study was to perform new experimental work on this issue by comparing palladium supported on both alumina and zirconia, submitted to either moderate (600 °C) or high (1000 °C) temperature treatments after preparation.

### EXPERIMENTAL

#### Catalyst preparation

Alumina Pural SB from Condea and a zirconia sample supplied by the *Politecnico di Milano* were used as supports and calcined at 600 °C before use. The impregnation of the supports was performed with a solution of palladium acetylacetonate (supplied by Merck) in toluene (Baker). The supports in powder form were suspended in a toluene solution and submitted to 24 h agitation in a rotating evaporator at room temperature. The solvent was then evacuated at 100 °C and final drying at 110 °C was performed under constant agitation. The dried material was then heat treated either at 600 or at 1000 °C under flowing air for 10 h. The samples were labelled P for palladium, and A and Z for alumina and zirconia carriers, respectively, and with a 6 or 10 when the final temperature of the heat treatment was 600 or 1000 °C, respectively. AP6 therefore denotes Pd/Al<sub>2</sub>O<sub>3</sub> heat treated at 600 °C at the end of the preparation.

\*e-mail: mlilian@ufba.br

### Characterization of catalysts

The surface area of the supports was measured using the BET method and adsorption equipment (ASAP 2000). Before analysis, the samples were out-gassed under a vacuum at 350 °C for 3 h.

XRD measurements were performed with a Shimadzu XRD-6000 apparatus. The following experimental conditions were used: 2θ range = 10-80°, step size = 0.02°, time per step = 4.80 s and CuKα radiation (λ = 1.5418 Å). The powder samples were analyzed without previous treatment. Palladium oxide crystallite sizes were estimated from the Debye Scherrer Equation using the measured width at half peak height of the PdO main diffraction peak (2θ = 33.88) for the 101 plan.

$$\tau_{PdO} = \frac{K\lambda}{b \cdot \cos\theta} \quad (1)$$

$\tau_{PdO}$  = PdO crystallite size ; λ = X-ray wavelength, 1.5418 Å for CuKα; θ = observed peak angle in degrees ; K = crystallite-shape factor ≈ 1 ; b = measured peak width in radians at half peak height.

XPS spectra were recorded with an Escalab VG MK1 spectrometer (Vacuum Generator) operating at a constant pass energy (50 eV), with an unmonochromated Mg Kα source (200 W) at a pressure of 10<sup>-8</sup> mbar. The binding energies of palladium species (BE) were referenced to that of the C 1s (285.0 eV).

The palladium content in the samples was measured by X-ray Fluorescence using a Shimadzu XRF 1800 apparatus.

The stability of the PdO<sub>x</sub> species was studied using the TPD technique. A total of 0.1 g catalyst diluted with 0.1 g of quartz powder was loaded in a quartz micro-reactor and heated in a He flow (30 mL/min) at a rate of 10 °C/min. Before TPD, the samples were heat treated under a flow of 5% O<sub>2</sub> in He, up to the initial calcining temperature and cooled down to room temperature under the same mixture. The O<sub>2</sub> Helium mixture was then changed to pure He and TDP initiated. O<sub>2</sub> release was monitored using a quadrupole mass spectrometer (Balzers QMS 200, m/e = 32).

The temperature-programmed catalytic tests (TPSR) were performed on a quartz micro-reactor loaded with 0.1 g catalyst diluted in 0.1 g quartz powder. The temperature of the reaction was measured by a K-type thermocouple located in a quartz compartment beside the catalyst bed. The samples were heated to either 600 or 1000 °C, under a flowing mixture of 0.5% CH<sub>4</sub>, 2% O<sub>2</sub> and 97.5% N<sub>2</sub> (100 mL/min) at a heating rate of 10 °C/min. Under the conditions applied, GHSV was close to 60000 h<sup>-1</sup>. Effluent gases were analyzed by mass spectrometry (Balzers QMS 200) and the following mass-to-charge ratios (m/e) were used to monitor the concentrations of products and reactants: CH<sub>4</sub> (m/e = 15 and 16), H<sub>2</sub>O (m/e = 18), CO (m/e = 28), O<sub>2</sub> (m/e = 32) and CO<sub>2</sub> (m/e = 44).

The conversion of methane was calculated using Equation 2, where C<sub>A</sub> represents the m/e = 15 signal recorded in the mass spectrometer (proportional to the methane concentration), C<sub>AO</sub> represents the m/e = 15 initial signal and X the methane conversion.

$$X = \frac{C_{Ao} - C_A}{C_{Ao}} = 1 - \frac{C_A}{C_{Ao}} \quad (2)$$

### RESULTS AND DISCUSSION

Table 1 shows the results for surface area, porosity and crystallinity of the supports.

From the data given in Table 1, the supports appeared to undergo significant transformation during the heat treatment between 600 and 1000 °C, as the surface area of both carriers shows a decrease by a factor of 3. Whereas the monoclinic structure of zirconia is maintained following the increase in temperature from 600 to 1000 °C, alumina exhibits structural transformation from γ phase to a mixture of θ, γ and δ phases. These results are in agreement with data from the literature.<sup>33,34</sup> In parallel, porous volume is reduced after calcining at 1000 °C, an observation also fully coherent with the reduction in surface area.

**Table 1.** Textural and crystallographic data for the alumina and zirconia supports, after heat treatment at 600 and 1000 °C

Sample	Surface area m <sup>2</sup> /g	Porous volume cm <sup>3</sup> /g	Crystalline phases
A6	179	0.5	γ-Al <sub>2</sub> O <sub>3</sub>
A10	63.2	0.31	γ-Al <sub>2</sub> O <sub>3</sub> , δ-Al <sub>2</sub> O <sub>3</sub> , θ-Al <sub>2</sub> O <sub>3</sub>
Z6	28.9	0.15	monoclinic
Z10	9.6	0.06	monoclinic*

\* Better crystallization

Table 2 shows the surface area of the catalysts, together with their porosity, and Pd content. Table 2 also shows Pd 3d<sub>5/2</sub> binding energy and values of Pd/Al and Pd/Zr, i.e. an estimation of the surface coverage of palladium for the different catalysts, as measured by XPS.

The data in Table 2 indicates that the surface area of the supported catalysts is close to that of the pure supports. This is an surprising since the impregnation method using an acetylacetonate precursor, in organic medium, cannot substantially alter the surface structure of the support as sometimes occurs when impregnation is performed under basic or acidic medium. Under such conditions, the support material can be partially leached thus, inducing a deposition on the carrier not only of the active phase, but also of the dissolved carrier species during the drying process. Further, the amount of palladium used, close to 1 wt %, is relatively small and similar for all four catalysts. Therefore, the present impregnation method cannot produce significant changes in the textural properties of the supports.

The Pd3d<sub>5/2</sub> binding energy values obtained by XPS are also shown in Table 2, indicating that Pd is predominantly in an oxidized form for all samples, corroborating previous reports.<sup>35-39</sup> Whether the PdO<sub>x</sub> are similar or differ among the present samples is hard to ascertain as the sensitivity of the equipment was limited. However, it is clear that the decrease in the surface palladium species disclosed by XPS

**Table 2.** Textural, chemical and XPS properties of supported Pd catalysts, heat treated at 600 and 1000 °C

Sample	Surface area (m <sup>2</sup> /g)	Porous volume (cm <sup>3</sup> /g)	Pd content (wt %)	BE Pd 3d <sub>5/2</sub> (eV)	Pd/Al or Pd/Zr
AP6	178	0.44	0.94	336.7	0.006
AP10	58	0.23	0.98	337.4	0.004
ZP6	33.2	0.14	0.95	336.6	0.064
ZP10	6	0.03	0.96	336.0	0.024

Pd content was measured by X-Ray Fluorescence, Pd 3d<sub>5/2</sub> binding energy (BE) and Pd/Al (Pd/Zr) were calculated from XPS data.

is much more pronounced than the decrease of the supports surface areas, as the values of the ratios Pd/Al or Pd/Zr decreased more than the surface area of the supports after the heat treatment at 1000 °C.

However, it is not known at this stage whether the decrease in Pd/Al (Pd/Zr) is simply due to the sintering of the palladium species, to a kind of SMSI<sup>40</sup> implying a migration of some support moieties on top of the palladium particles, or both these effects. Although generally crystallite sizes and particle sizes are not simply correlated, the crystallite sizes of PdO<sub>x</sub> were calculated using the Debye-Scherrer equation applied to the PdO main diffraction peak ( $2\theta = 34^\circ$ ) in all catalysts.

Figure 1 shows the deconvolution of the XRD profile close to the [101] line of PdO at  $2\theta = 34^\circ$ . In this case, the mean crystallite size for PdO<sub>x</sub> was estimated to be 28 and 36 nm for ZP6 and ZP10, respectively, a less pronounced variation than that estimated through the variations of Pd/Zr. In other words, the thermal treatment at 1000 °C seems to induce both a sintering of PdO<sub>x</sub> and partial covering of the PdO<sub>x</sub> by zirconia moieties. Similar patterns were also observed in alumina samples, although in this case the deconvolution was of limited quality, due to interferences between alumina and PdO<sub>x</sub> lines.

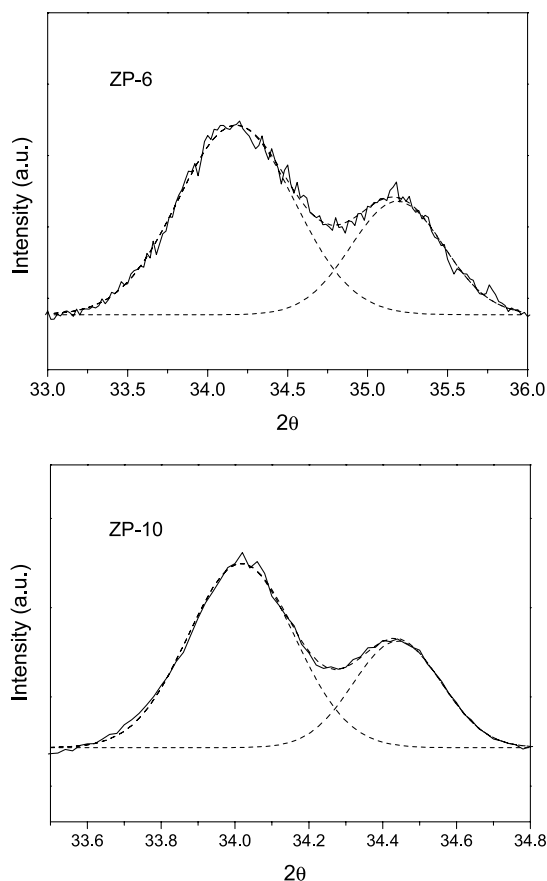


**Figure 1.** Window of XRD spectrum where the [101] line of PdO appears for ZP-6 and ZP-10 catalysts. Deconvolution of the experimental spectrum (dash lines); experimental spectrum (solid lines)

Figure 2 shows the TPD spectra of AP6, AP10, ZP6 and ZP10. In all cases, PdO<sub>x</sub> species appear stable up to 570-580 °C, and fully decomposed above 900-950 °C, values in strong agreement with literature data.<sup>31,32</sup> The maximum decomposition temperature was 791, 733, 847 and 722 °C, for AP6, AP10, ZP6 and ZP10 respectively. Two main points warrant closer analysis. The first is the fact that PdO<sub>x</sub> is less stable after heat treatment of the catalysts at 1000 °C than after a calcining temperature of 600 °C. After calcining

at 1000 °C, the temperature at the beginning of PdO<sub>x</sub> decomposition is lower or similar to the value after heat treatment at 600 °C, while the temperature at the end of the decomposition is also significantly decreased. This implies that the particles of PdO<sub>x</sub> are less stable when their size increases, or that their interaction with the support is more limited. Regardless of the exact reason, the instability domain for the PdO<sub>x</sub> species must influence the results of the catalytic methane combustion.

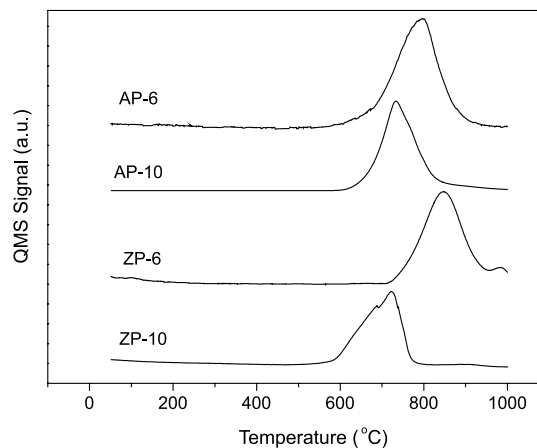


**Figure 2.** Oxygen TPD profile, under He flow, for the catalysts AP-6, AP-10, ZP-6 and ZP-10

The second point relates to the comparison between alumina- and zirconia-supported palladium. PdO<sub>x</sub> species supported on zirconia have been observed to be much less stable than on alumina by Farrauto *et al.*<sup>41</sup> The present results showed that this is not always the case and that the history of the catalysts, nature of the support, as well as the preparation method, all influence the behavior of PdO<sub>x</sub> entities, implying that the definition of an optimized catalyst for methane combustion is rather more complex.

Figures 3 and 4 depict the TPSR curves for the 4 catalysts. For experimental reasons, the TPSR was stopped at 600 °C for the AP6 and ZP6 catalysts, but was continued up to 1000 °C for the samples AP10 and ZP10.

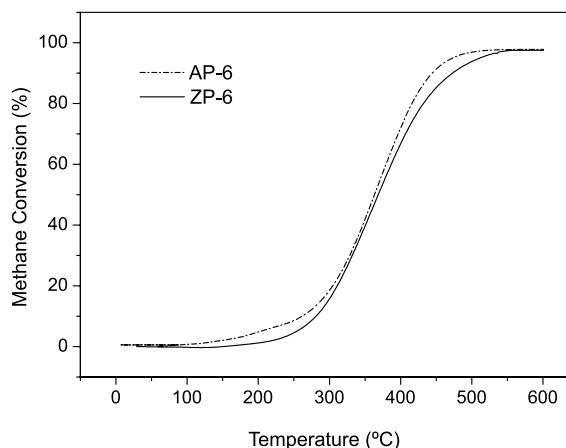


**Figure 3.** TPSR curves of the catalysts ZP-6 and ZP-10 during methane combustion

The relation between conversion of methane and temperature increase is very different in both cases. Reiterating, the lower the temperature required to reach a given conversion, the more active

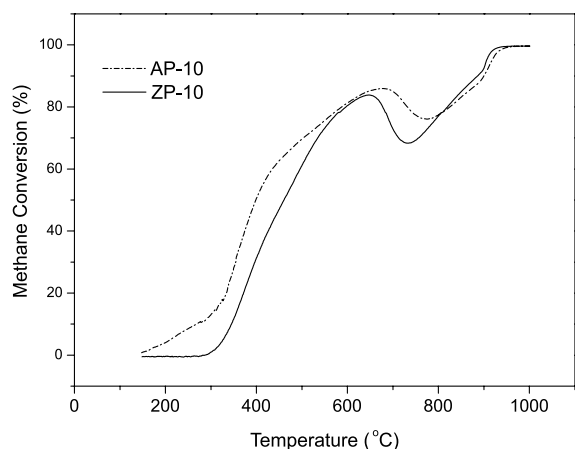


**Figure 4.** TPSR curves of the catalysts AP-6 and AP-10 during methane combustion

the catalyst. For AP6 and ZP6, the two curves are fairly similar although the AP6 sample is more active than the ZP6 over the whole temperature range. This is evidenced by the values given in Table 3, showing the temperatures at which conversions are 10, 50 and 80% respectively.

**Table 3.** Temperatures observed at CH<sub>4</sub> iso-conversion (10, 50 and 80% respectively) obtained by TPSR technique in Figures 3 and 4, for the AP6, ZP6, AP10 and ZP10 catalysts

Catalyst	T <sub>10%</sub> (°C)	T <sub>50%</sub> (°C)	T <sub>80%</sub> (°C)
AP6	248	340	412
ZP6	270	350	420
AP10	250	395	600; 720; 830*
ZP10	300	405	585; 670; 800*

T<sub>x%</sub> = Temperature observed for x% methane conversion. \*The three different temperatures noted at 80% conversion for AP-10 and ZP-10 are due to the decrease followed by an increase of conversion in the high temperature range.

Comparing the conversion to the stability of PdO<sub>x</sub> as measured by oxygen TPD revealed that the whole conversion occurs over a temperature range in which PdO<sub>x</sub> is completely stable for both AP6 and ZP6. Due to the high activity observed, no clear difference can be seen between the two catalysts under the experimental conditions applied.

The situation is more complex concerning the catalysts heat treated at 1000 °C before catalytic measurements. The first point worthy of comment is the fact that both catalysts were less active than preceding ones, as an increase of at least 30 to 40 °C is required to achieve 50% conversion. Furthermore, above around 400 °C, the increase in conversion when increasing temperature is slowed down, and above approximately 650 °C, as seen in the literature,<sup>31,32</sup> causes a drop in activity. Between 630 and around 830 °C, activity is lower than that obtained at 625 °C. Whereas AP10 is more active than ZP10 up to 500 °C, the opposite is true at temperatures between 625 and 900 °C (see T = 80% conversion in Table 3).

The decrease in conversion at increasing temperatures has been observed in numerous studies and was attributed to the decomposition of PdO<sub>x</sub> species to metallic palladium, a much less active substance than PdO<sub>x</sub> over this temperature range. The same interpretation holds for the present results. However, it is notable here that despite slightly better activity of ZP10 in comparison with AP10 between 500 and 625 °C, the drop in activity is more rapid with this catalyst

than with AP10, between 625 and 700 °C. Examining the oxygen TPD curves of Figure 2 reveals that PdO<sub>x</sub>/ZP10 decomposes more easily than PdO<sub>x</sub>/AP10, an observation in complete agreement with catalytic behavior. Although much less sophisticated than the *in situ* experiments of Grunwaldt *et al.*<sup>31</sup> the findings of the present experiments using simple oxygen TPD are in complete agreement with the observations of these authors.

A further point for analysis upon observing the conversion curves versus temperature for catalysts AP10 and ZP10 is that at temperatures above about 400 °C, the increase in conversion with temperature increase is less efficient than expected from an exponential conversion increase versus temperature. This suggests that above 400 °C physical transformations of the catalysts tested occur. We may speculate that over this temperature range PdO<sub>x</sub> particles begin to transform into metallic Pd, leading to a decrease in the active area of PdO<sub>x</sub>.<sup>1,3,10,18</sup> The whole transformation is accomplished when the TPSR curves were at their minimum above temperatures of 700 °C. The further activity increase above this temperature is due to the fact that metallic Pd particles are now the main active species, whose activity increases with temperature as expected. The differences in the PdO<sub>x</sub> stability temperature range when comparing the oxygen TPD curves and the anomalous behavior of the catalysts on TPSR curves is probably due to differences in oxidizing potential of the atmosphere surrounding the Pd/PdO<sub>x</sub> species in both experiments.

Finally, it was observed that at temperatures higher than 500 °C, the ZP10 catalyst is more active than the AP10 sample. Taken together with the difference in PdO<sub>x</sub> stability discussed previously, it is possible to deduce that some oxygen species of the zirconia support is involved in the catalytic process, through a kind of bulk oxygen migration<sup>28</sup> mediated by the palladium species. Such a phenomenon cannot exist with the alumina support because oxygen is very strongly bound to aluminum.

## CONCLUSIONS

The present study has shown that the palladium catalysts prepared through impregnation with palladium acetylacetonate are quite active in the conversion of methane, especially at low temperatures, and particularly when the catalysts have been heat treated before use at a temperature of around 600 °C. An increase in the preparation temperature to 1000 °C generates catalysts with a lower PdO<sub>x</sub> active area that are less active than the catalysts prepared at 600 °C under the reaction conditions applied in this work. A clear pattern appears between PdO<sub>x</sub> stability and activity, mainly over the temperature range in which PdO<sub>x</sub> showed instability. The present results suggest that it is possible to modify PdO<sub>x</sub> stability by for example, changing the size of PdO<sub>x</sub> particles and their support, at least at temperatures lower than 600 °C, and also that TPD of oxygen during the decomposition of PdO<sub>x</sub> is a powerful tool for optimizing this family of combustion catalysts.

## ACKNOWLEDGMENTS

R. Frety thanks FAPESB (Fundação de Apoio à Pesquisa do Estado da Bahia) for a grant during the period 2009-2010 and CNPq for a grant during a 6 months period in 2011.

## REFERENCES

- Groppi, G.; Cristiani, C.; Lietti, L.; Ramella, C.; Valentini, M.; Forzatti, P.; *Catal. Today* **1999**, *50*, 399.
- Geus, J. W.; Van Giezen, J. C.; *Catal. Today* **1999**, *47*, 169.
- Centi, G.; *J. Mol. Catal. A: Chem.* **2001**, *173*, 287.

4. Choudhary, T. V.; Banerjee, S.; Choudhary, V. R.; *Appl. Catal., A* **2002**, *234*, 1.
5. Forzatti, P.; *Catal. Today* **2003**, *83*, 3.
6. Gélín, P.; Urfels, L.; Primet, M.; Tena, E.; *Catal. Today* **2003**, *83*, 45.
7. Ciuparu, D.; Lyubovsky, M. R.; Altman, E.; Pfefferle, L. D.; Datye, A.; *Catal. Rev.* **2002**, *44*, 593.
8. Deng, Y.; Nevell, T. G.; *Catal. Today* **1999**, *47*, 279.
9. Kucharczyk, B.; Tylus, W.; Kepinski, L.; *Appl. Catal., B* **2004**, *149*, 27.
10. Gélín, P.; Primet, M.; *Appl. Catal., B* **2002**, *9*, 1.
11. Simplício, L. M. T.; Brandão, S. T.; Sales, E. A.; Lietti, L.; Bozon-Verduraz, F.; *Appl. Catal., B* **2006**, *63*, 9.
12. Ribeiro, F. H.; Chow, M.; Dalla Beta, R. A.; *J. Catal.* **1994**, *146*, 537.
13. Escandón, L. S.; Ordóñez, S.; Vega, A.; Díez, F. V.; *Chemosphere* **2005**, *58*, 9.
14. Eguchi, K.; Arai, H.; *Appl. Catal., A* **2001**, *222*, 359.
15. Sekizawa, K.; Widjaja, H.; Maeda, S.; Ozawa, Y.; Eguchi, K.; *Catal. Today* **2000**, *59*, 69.
16. Sekizawa, K.; Widjaja, H.; Maeda, S.; Ozawa, Y.; Eguchi, K.; *Appl. Catal., A* **2000**, *200*, 211.
17. Yoshida, H.; Nakajima, T.; Yazawa, Y.; Hattori, T.; *Appl. Catal., B* **2007**, *71*, 70.
18. Simplício, L. M. T.; Brandão, S. T.; Domingos, D.; Bozon-Verduraz, F.; Sales, E. A.; *Appl. Catal., A* **2009**, *360*, 2.
19. Colussi, S.; Trovarelli, A.; Cristiani, C.; Lietti, L.; Groppi, G.; *Catal. Today* **2011**, *180*, 124.
20. Carstens, J. N.; Su, S. C.; Bell, A. T.; *J. Catal.* **1998**, *176*, 136.
21. Guerrero, S.; Araya, P.; Wolf, E. E.; *Appl. Catal., A* **2006**, *298*, 243.
22. Specchia, S.; Finocchio, E.; Busca, G.; Palmisano, P.; Specchia, V.; *J. Catal.* **2009**, *263*, 134.
23. Yang, S.; Valiente, A. M.; Gonzales, M. B.; Ramos, T. R.; Ruiz, A. G.; *Appl. Catal., B* **2000**, *28*, 223.
24. Hoflund, G. B.; Zhenhua, L.; Epling, W. S.; Göbel, T.; Schneider, P.; Hahn, H.; *Catal. Lett.* **2000**, *70*, 97.
25. Muller, C. A.; Maciejewski, M.; Koeppel, R. A.; Baiker, A.; *J. Catal.* **1997**, *166*, 36.
26. Su, S. C.; Carstens, J. N.; Bell, A. T.; *J. Catal.* **1998**, *176*, 125.
27. Fujimoto, K.; Ribeiro, F. H.; Borja, M. A.; Iglesia, E.; *J. Catal.* **1998**, *179*, 431.
28. Muller, C. A.; Maciejewski, M.; Koeppel, R. A.; Baiker, A.; *Catal. Today* **1999**, *47*, 245.
29. Hicks, R. F.; Qi, H.; Young, M. L.; Lee, R. G.; *J. Catal.* **1990**, *122*, 280.
30. Lyubovsky, M.; Pfefferle, L.; *Appl. Catal., A* **1998**, *173*, 107.
31. Grunwaldt, J. -D.; van Vegten, N.; Baiker, A.; *Chem. Commun.* **2007**, *44*, 4635.
32. van Vegten, N.; Maciejewski, M.; Krumeich, F.; Baiker, A.; *Appl. Catal., B* **2009**, *93*, 38.
33. Thevenin, P. O.; Pocaroba, E.; Pettersson, L. J.; Karhu, H.; Vayrynen, I. J.; Jaras, S. G.; *J. Catal.* **2002**, *207*, 139.
34. Church, J. S.; Cant, N. W.; Trimm, D. L.; *Appl. Catal., A* **1993**, *101*, 105.
35. Voogt, E. H.; Mens, A. J. M.; Gijzeman, O. L. J.; Geus, J. W.; *Surf. Sci.* **1996**, *350*, 21.
36. Voogt, E. H.; Mens, A. J. M.; Gijzeman, O. L. J.; Geus, J. W.; *Catal. Today* **1999**, *47*, 321.
37. Brun, M.; Berthet, A.; Bertolini, J. C.; *J. Electron Spectrosc. Relat. Phenom.* **1999**, *104*, 55.
38. Suhonen, S.; Valden, M.; Pessa, M.; Savimaki, A.; Harkonen, M.; Hietikko, M.; Pursiainen, J.; Laitinen, R.; *Appl. Catal., A* **2001**, *207*, 113.
39. Sohn, J. M.; Kang, S. K.; Woo, S. I.; *J. Mol. Catal. A: Chem.* **2002**, *186*, 135.
40. Hoang, D. L.; Lieske, H.; *Catal. Lett.* **1994**, *27*, 33.
41. Farrauto, R. J.; Lampert, J. K.; Hobson, M. C.; Waterman, E. M.; *Appl. Catal., B* **1995**, *6*, 263.